

1       **“Intrauterine growth restriction is associated with cardiac ultrastructural and**  
2       **gene expression changes related to the energetic metabolism in a rabbit model”**

3  
4       Anna Gonzalez-Tendero<sup>1</sup>, Iratxe Torre,<sup>1,2</sup> Patricia Garcia-Canadilla<sup>1,3</sup>, Fátima  
5       Crispi<sup>1,2,4</sup>, Francisco García-García<sup>5,6,7</sup>, Joaquin Dopazo<sup>5,6,7</sup>, Bart Bijmens<sup>3</sup>, Eduard  
6       Gratacós<sup>1,2,4</sup>.

7  
8       <sup>1</sup> Fetal and Perinatal Medicine Research Group, Institut d'Investigacions Biomèdiques  
9       August Pi i Sunyer (IDIBAPS), University of Barcelona, Barcelona, Spain; <sup>2</sup> Centro de  
10       Investigación Biomédica en Red de Enfermedades Raras (CIBERER), Hospital Clinic-  
11       University of Barcelona, Barcelona, Spain; <sup>3</sup> ICREA-PhySense, N-RAS, Universitat  
12       Pompeu Fabra, Barcelona, Spain; <sup>4</sup> Department of Maternal-Fetal Medicine, Institut  
13       Clínic de Ginecologia, Obstetrícia i Neonatologia (ICGON), Barcelona, Spain;  
14       <sup>5</sup>Bioinformatics Department, Centro de Investigación Principe Felipe (CIPF), Valencia,  
15       Spain; <sup>6</sup> Functional Genomics Node, INB, CIPF, Valencia, Spain; <sup>7</sup> Centro de  
16       Investigación Biomédica en Red de Enfermedades Raras (CIBERER), CIPF, Valencia,  
17       Spain.

18  
19       **Author contributions**

20  
21       A.G.T carried out the major part of the experimental work and wrote the paper. P.G.C.  
22       provided the GUI (Graphical User Interface) designed in MatLab. I.T. performed the  
23       gene expression experiments. A.G.T, I.T, F.C. and E.G. contributed to the conception  
24       and design of the experiments. J.D. and F.G.G. performed the bioinformatics analysis of  
25       the gene expression microarrays. I.T., F.C., B.B., E.G. and A.G.T. contributed in the  
26       collection, analysis and interpretation of data as well as the drafting and revising of the  
27       article. All authors discussed the results, commented on the manuscript and approved  
28       the version to be published. All persons designated as authors qualify as authorship, and  
29       all those who qualify for authorship are listed.

30  
31       **Running head:**

32       Cardiac structural and energetic changes in IUGR.

33  
34       **Correspondence:**

35  
36       Eduard Gratacós MD, PhD.  
37       Fetal and Perinatal Medicine Research Group, IDIBAPS  
38       Department of Maternal-Fetal Medicine, ICGON  
39       Hospital Clinic – Universitat de Barcelona  
40       Sabino de Arana, 1  
41       08028 Barcelona, Spain.  
42       Ph. (+34) 93 227 9333  
43       Fax. (+34) 93 227 9336  
44       e-mail: GRATACOS@clinic.ub.es

45

46 **ABSTRACT**

47 Intrauterine growth restriction (IUGR) affects 7-10% of pregnancies and is associated  
48 with cardiovascular remodeling and dysfunction which persists into adulthood. The  
49 underlying subcellular remodeling and cardiovascular programming events are still  
50 poorly documented. Cardiac muscle is central in the fetal adaptive mechanism to IUGR  
51 given its high energetic demands. The energetic homeostasis depends on the correct  
52 interaction of several molecular pathways and the adequate arrangement of intracellular  
53 energetic units (ICEUs), where mitochondria interact with the contractile machinery and  
54 the main cardiac ATPases to enable a quick and efficient energy transfer. We studied  
55 subcellular cardiac adaptations to IUGR in an experimental rabbit model. We evaluated  
56 the ultrastructure of ICEUs with transmission electron microscopy and observed an  
57 altered spatial arrangement in IUGR, with significant increases in cytosolic space  
58 between mitochondria and myofilaments. A global decrease of mitochondrial density  
59 was also observed. In addition, we conducted a global gene expression profile by  
60 advanced bioinformatics tools to assess the expression of genes involved in the  
61 cardiomyocyte energetic metabolism, and identified four gene modules with a  
62 coordinated over-representation in IUGR: oxygen homeostasis (GO: 0032364),  
63 mitochondrial respiratory chain complex I (GO:0005747), oxidative phosphorylation  
64 (GO: 0006119) and NADH dehydrogenase activity (GO:0003954). These findings  
65 might contribute to changes in energetic homeostasis in IUGR. The potential  
66 persistence and role of these changes in long term cardiovascular programming deserves  
67 further investigation.

68 **Keywords:**

69 Cardiomyocyte intracellular organization; Energetic metabolism; Fetal cardiac  
70 programming; Intracellular energetic units; Intrauterine growth restriction.

71

## 72 **1. Introduction**

73 Intrauterine growth restriction (IUGR), due to placental insufficiency, affects up to 7-  
74 10% of pregnancies and is a major cause of perinatal mortality and long-term morbidity  
75 (1). Low birth weight, most likely due to IUGR is strongly associated with increased  
76 risk of cardiovascular mortality in adulthood (7). This association is thought to be  
77 mediated through fetal cardiovascular programming. IUGR fetuses suffer from a  
78 chronic restriction of oxygen and nutrients (47), which triggers the initiation of a variety  
79 of adaptive structural (12, 14, 46, 51) and metabolic responses (25) due to a  
80 pressure/volume overload and subsequently, with the objective of providing a more  
81 efficient myocardial performance. As a consequence, IUGR fetuses and newborns show  
82 signs of cardiovascular remodeling and altered function (21, 13, 14).

83 The effect of hypoxia and nutrient restriction during pregnancy in cardiac development  
84 and function has been previously studied, demonstrating the association of IUGR to a  
85 cardiac remodeling. Maternal hypoxia has been related to changes in cardiac structure  
86 and function (37, 38, 49), increased cardiac collagen content (50), changes in  
87 cardiomyocyte proliferation and apoptosis (6, 28) and to long-term effects increasing  
88 cardiac susceptibility to ischemia-reperfusion injury by causing changes on myocardial  
89 energetic metabolism (39, 55). However, the underlying events of cardiac remodeling in  
90 IUGR at subcellular scale still remain poorly understood. The heart is an organ with  
91 high-energy requirements in the form of ATP to ensure proper functioning (29).  
92 Efficient energetic homeostasis depends on the correct arrangement of subcellular  
93 organelles. A close spatial interaction between mitochondria and the sarcomere  
94 contractile filaments is essential to ensure adequate and quick transportation of ATP.  
95 This is reached by the intracellular energetic units (ICEUs), that are structural and  
96 functional units, consisting of mitochondria located at the level of the sarcomeres  
97 between Z-lines interacting with surrounding myofilaments, sarcoplasmic reticulum,

98 cytoskeleton and cytoplasmic enzymes, that promote an endogenous cycling of adenine  
99 nucleotides between mitochondria and ATPases (40, 44, 45). Alterations in ICEUs  
100 arrangement together with an impaired local energetic regulation of the main cardiac  
101 ATPases have been described in cardiac pathophysiological processes (24). In addition,  
102 cardiomyocyte energetic homeostasis is regulated by a complex interaction of molecular  
103 pathways, mainly involving energy production through oxidative phosphorylation in the  
104 mitochondria (48). It has been widely described that disruption of mitochondrial  
105 oxidative phosphorylation plays a critical role in the development of heart failure (26,  
106 35, 52). The oxidative phosphorylation takes place in the mitochondrial electron  
107 transport chain. It is composed of five complexes; in the complex I the enzyme NADH  
108 dehydrogenase catalyzes the reaction (2). Deficiencies in complex I function have been  
109 observed in dilated cardiomyopathy and in failing myocardium (41).

110 The goal of the present work was to evaluate the impact of chronic oxygen and nutrient  
111 restriction during a critical period for cardiac development, as present in IUGR, with  
112 regard to cardiomyocyte intracellular organization and gene expression of key pathways  
113 for energy production. For this purpose, the cardiomyocyte intracellular organization  
114 was studied by transmission electron microscopy. Additionally, the functional  
115 interpretation of the global gene expression profile was studied by means of advanced  
116 bioinformatics tools. The data presented here show changes in the cardiomyocyte  
117 intracellular organization in IUGR, specifically affecting ICEUs, together with an  
118 abnormal up-representation of blocks of genes acting together in a coordinated way,  
119 related to the cardiac oxygen homeostasis and energy production.

120

121

122

123

## 124 2. Material and methods

### 125 2.1 Animal Model

126 New Zealand white rabbits were provided by a certified breeder. Dams were housed for  
127 1 week before surgery in separate cages on a reversed 12/12 h light cycle. Animals were  
128 fed a diet of standard rabbit chow and water *ad libitum*. Animal handling and all  
129 procedures were performed in accordance to applicable regulations and guidelines and  
130 with the approval of the Animal Experimental Ethics Committee of the University of  
131 Barcelona.

132 Six New Zealand White pregnant rabbits were used to reproduce a model of IUGR,  
133 following the method previously described (16, 17). At 25 days of gestation, selective  
134 ligation of uteroplacental vessels was performed as previously described (16, 17).  
135 Briefly, tocolysis (progesterone 0.9 mg/kg intramuscularly) and antibiotic prophylaxis  
136 (Penicillin G 300.000 UI intravenous) were administered prior surgery. Ketamine 35  
137 mg/kg and xylazine 5 mg/kg were given intramuscularly for anesthesia induction.  
138 Inhaled anesthesia was maintained with a mixture of 1-5% isoflurane and 1-1.5 L/min  
139 oxygen. After a midline laparotomy, both uterine horns were exteriorized. The number  
140 of gestational sacs from each horn were counted and numbered. Pregnant rabbits have  
141 between 4 and 7 gestational sacs per horn. At random, one horn was assigned as the  
142 IUGR horn and the other horn was considered as the normal control growth. In all  
143 gestational sacs from the horn assigned as IUGR, a selective ligation of the 40-50% of  
144 the uteroplacental vessels was performed. No additional procedure was performed in the  
145 horn assigned as control. After the procedure, the abdomen was closed and animals  
146 received intramuscular meloxicam 0.4 mg/kg/24 h for 48 h, as postoperative analgesia.  
147 Five days after surgery, at 30 days of gestation, a caesarean section was performed  
148 under the same anesthetic procedure and all living rabbit kits and their placentas were  
149 identified and weighted. Kits were anesthetized with an injection of ketamine and

150 xylazine. Following surgical removal from the chest cavity, hearts for gene expression  
151 analysis were immediately snap-frozen and stored at -80°C until the moment of use.  
152 Hearts for transmission electron microscopy imaging were processed as described in  
153 section 2.2.1.

154

## 155 2.2 Electron Microscopy

### 156 2.2.1 Tissue processing

157 Hearts from 3 control and 3 IUGR rabbit fetuses, each control-IUGR pair coming from  
158 a different litter, were arrested in an ice-cold  $\text{Ca}^{2+}$ -free phosphate saline buffer  
159 immediately after surgical removal from the chest cavity. Random areas of left ventricle  
160 were dissected and cut into small pieces. Approximately 10 pieces from each left  
161 ventricle were incubated with 2% paraformaldehyde and 2.5% glutaraldehyde in  
162 phosphate buffer (PB) during 24 hours at 4°C. Then, tissue pieces were washed with a  
163 PB buffer and post-fixed with 1% osmium tetroxide in PB containing 0.8% potassium  
164 ferricyanide at 4°C for 2 hours. Next, samples were dehydrated in acetone, infiltrated  
165 with Epon resin during 2 days, embedded in the same resin and polymerized at 60°C  
166 during 48 hours. Semi-thin 500 nm sections were made in order to confirm the  
167 longitudinal orientation of cardiac sarcomeres under light microscope. Subsequently, 50  
168 nm ultra-thin sections were cut using a Leica UC6 ultramicrotome (Leica  
169 Microsystems, Vienna, Austria) and mounted on Formvar-coated copper grids. Sections  
170 were stained with 2% uranyl acetate in water and lead citrate. Tissue sections were  
171 imaged using a JEM-1010 electron microscope (Jeol, Japan) equipped with a CCD  
172 camera Megaview III and the AnalySIS software (Soft Imaging System GmbH, 1998).

173

174

175

176 *2.2.2 Morphological analysis*

177 Morphological analysis of intracellular cardiomyocyte organization was performed in 2  
178 randomly chosen left ventricle tissue pieces, from each subject. For each tissue piece, 50  
179 nm ultra-thin sections were obtained from two ventricular areas separated 1  $\mu\text{m}$  of  
180 distance. Images were taken at 20000x magnification when an area containing  
181 longitudinal myofilaments surrounded by a mitochondrial network was observed. In this  
182 study, micrographs with disrupted mitochondria, disrupted sarcomeres or transversal or  
183 oblique orientation of sarcomeres were excluded from the quantification. Electron  
184 micrographs were taken and quantified in a blinded fashion and by one researcher  
185 (A.G.T.). Images were analyzed from three viewpoints:

186

187 *General cardiomyocyte cytoarchitecture: volume density estimation*

188 The volume densities of myofilaments, mitochondria and cytoplasm were estimated in  
189 10 electron micrographs acquired from each heart. For this purpose, a grid in which  
190 each line intersection served as a sample point was generated on each image using  
191 Image J (36), according to standard stereological methods (20). Volume densities of the  
192 different structures were calculated by counting the number of points hitting the studied  
193 structures divided by the total number of points hitting the section, using a grid size of  
194 0.02 a.u.

195

196 *Mitochondrial area and number*

197 The area of individual mitochondria was determined from 193 mitochondria in each  
198 study group. Individual mitochondria were delineated and their area was measured  
199 using the AnalySIS software. The number of mitochondria was counted by using 10  
200 randomly chosen images from each heart as previously described (22).

201

## 202 *ICEUs arrangement*

203 The cytoplasmic area and the mean distance between mitochondria and myofilaments  
204 within ICEUs were measured by delineating the area of cytoplasm existing between two  
205 consecutive z-disks and the immediately adjacent mitochondria, as shown in Fig.1,  
206 using a custom-made GUI (Graphical User Interface) designed in MatLab (30). The  
207 area was automatically calculated and the mean distance between mitochondria and  
208 myofilaments within ICEUs was obtained by evaluating the Euclidean distance of the  
209 delineated region (11). A total of 169 ICEUs were analyzed in the control group,  
210 whereas 154 ICEUs were analyzed in the IUGR group, obtained from 10 to 15 electron  
211 micrographs from each heart. We analyzed all the ICEUs found in the transmission  
212 electron microscopy images. However, ICEUs were discarded from the quantification  
213 when they were not clear, blurred or if the limits to mitochondria were not sharp  
214 enough.

215

## 216 2.3 Gene set expression analysis

### 217 *2.3.1 Gene expression microarray*

218 The IUGR-gene expression profile was analyzed in 6 control and 6 IUGR rabbit fetuses,  
219 each control-IUGR pair coming from a different litter. In this study, special attention  
220 was paid to the expression profile of groups of genes related to energetic metabolism.  
221 Total RNA was isolated from 40 mg of each left ventricle. The extraction protocol was  
222 a combination of TRIzol as reagent and the RNeasy Mini kit (Qiagen). For each sample  
223 included in the study, the total amount of RNA was always above 25  $\mu\text{g}$  with  
224 homogenous profile, showing a RNA integrity number between 9.3 to 9.9 (analyzed  
225 with RNA 6000 Nano and Bioanalyzer 2100; Agilent). Next, 500 ng of total RNA from  
226 each sample were labeled with the Quick Amp One-color Labelling kit (Agilent) and  
227 fluorochrome Cy3. Efficiency of labeling (Cy3pmol/ $\mu\text{g}$ ) was analyzed using a



228 Nanodrop spectrophotometer to check that values were above the minimum  
229 requirements ( $>1.65 \mu\text{g}$  and  $> 9.0 \text{ pmols Cy3/} \mu\text{g}$ ). Additionally, a RNA 6000 Nano  
230 mRNA assay in the Bioanalyzer 2100 was done in order to assess that all the samples  
231 show a comparable profile and fragments size was as expected (200-2000 bp). Then,  
232 1650  $\mu\text{g}$  of RNA obtained from each labeled sample were hybridized during 17 hours at  
233  $65^\circ\text{C}$  with a Rabbit Microarray (Agilent Microarray Design ID 020908) containing  
234 43,803 probe sequences obtained from the rabbit genome. All probe sequences included  
235 in the microarray were based on rabbit (*Oryctolagus cuniculus*) public transcript data.  
236 Finally, hybridization was quantified at  $5 \mu\text{m}$  resolution (Axon 4000B scanner). Data  
237 extraction was done using Genepix Pro 6.0 software and results were subjected to  
238 bioinformatics analysis.

239

### 240 2.3.2 Gene set analysis

241 Gene set analysis was carried out for the Gene Ontology (GO) terms using the FatiScan  
242 (3) algorithm, implemented in the Babelomics suite (4). This method detects  
243 significantly up- or down-regulated blocks of functionally related genes in lists of genes  
244 ordered by differential expression. FatiScan can search for modules of genes that are  
245 functionally related by different criteria such as common annotations like GO terms.

246 The FatiScan algorithm studies the distribution of functional terms across the list of  
247 genes coming from the microarray experiment, extracting significantly under- and over-  
248 represented GO terms in a set of genes. GO terms were grouped in three categories: 1)  
249 cellular components, that refer to the place in the cell where a gene product is active; 2)  
250 biological processes, which refer to a biological objective to which a gene or gene  
251 product contributes and 3) molecular functions; that represent all the biochemical  
252 activities of a gene product. FatiScan uses a Fisher's exact test for  $2 \times 2$  contingency  
253 tables for comparing two groups of genes and extracting a list of GO terms whose

254 distribution among the groups is significantly different. Given that many GO terms are  
255 simultaneously tested, the results of the test are corrected for multiple testing to obtain  
256 an adjusted p-value. FatiScan returns adjusted p-values based the False Discovery Rate  
257 (FDR) method (10). GO annotation for the genes in the microarray were taken from  
258 the Blast2GO Functional Annotation Repository web page  
259 (<http://bioinfo.cipf.es/b2gfar/>). The raw microarray data have been deposited in the  
260 Gene Expression Omnibus database under accession number GSE37860.

261

## 262 2.4 Statistical analysis

263 Statistical analysis of the morphological study was performed with the statistical  
264 package SPSS 18.0 (SPSS, Chicago). Data are expressed as mean  $\pm$  SD or median  
265 (interquartile range, IQR). Statistical significance of differences between experimental  
266 groups was compared with an unpaired two-tailed t-test or Mann-Whitney test,  
267 depending whether variables followed a normal distribution or not. Differences were  
268 considered significant with probability values of  $p < 0.05$ . Statistical methods concerning  
269 gene expression analysis have been detailed on section 2.3.2.

270

## 271 3. Results

### 272 3.1 Animal model of IUGR: fetal biometry

273 Table 1 summarizes biometric outcome of the study groups. Birth weight, placental  
274 weight, heart weight, crown-rump length and abdominal girth decreased significantly in  
275 IUGR kits compared to normally growth kits. Additionally, heart to body weight ratio  
276 was increased in the IUGR group.

277

278

279

## 280 3.2 Morphological analysis

### 281 3.2.1 Intracellular arrangement

282 Significant differences between IUGR and normally growth fetal myocardium could be  
283 observed regarding the arrangement of the intracellular components. A representative  
284 image of this is displayed in Fig. 2A-B, showing that IUGR rabbits present a looser  
285 packing of mitochondria and an increased cytosolic space between mitochondria and  
286 myofilaments. Quantification of the volume densities of myofilaments, mitochondria  
287 and cytoplasm is shown in Fig.2C. Stereological examination of micrographs obtained  
288 from control and IUGR myocardium showed that the amount of myofilaments was not  
289 different between control and IUGR rabbits (mean  $34.64 \pm \text{SD } 4.04\%$  in control vs.  
290  $34.74 \pm 6.01\%$  in IUGR,  $p=0.973$ ). On the other hand, changes in the relative volume  
291 occupied by mitochondria and cytoplasm were observed among control and IUGR  
292 myocardium. The relative volume occupied by mitochondria was significantly  
293 decreased in IUGR fetuses ( $34.59 \pm 4.23\%$  in control vs.  $27.74 \pm 5.28\%$  in IUGR,  
294  $p=0.032$ ), while the relative volume occupied by total cytoplasm was significantly  
295 increased under IUGR ( $30.77 \pm 3.04\%$  in control vs.  $37.53 \pm 4.97\%$  in IUGR,  $p=0.018$ ).  
296 In this study we classified the cytoplasm into two categories according to its  
297 localization: i) cytoplasm located between mitochondria and myofilaments (ICEUs) and  
298 ii) cytoplasm not located in the ICEUs, namely free cytoplasm. The cytoplasm existing  
299 within ICEUs was significantly increased under IUGR ( $6.47 \pm 0.1.18\%$  in control vs.  
300  $8.69 \pm 1.75\%$  in IUGR,  $p=0.027$ ). However, the free cytoplasm was not altered ( $24.31 \pm$   
301  $2.91\%$  in control vs.  $28.84 \pm 5.27 \%$  in IUGR,  $p=0.095$ ).

302

### 303 3.2.2 Mitochondria: area and number

304 The average area of individual mitochondria as well as the number of mitochondria  
305 were quantified in order to test whether changes described in section 3.2.1 could be due

306 to changes in the mitochondrial size or number (Fig.3). Results did not show  
307 statistically significant differences regarding the area of individual mitochondria  
308 ( $0.3094 \pm 0.0595 \mu\text{m}^2$  in control vs.  $0.2407 \pm 0.0176 \mu\text{m}^2$  in IUGR;  $p=0.128$ ). Average  
309 number of mitochondria neither resulted to be different between control and IUGR  
310 hearts ( $27.47 \pm 9.32$  in control vs.  $26.33 \pm 8.06$  in IUGR;  $p=0.627$ ).

311

### 312 3.2.3 ICEUs arrangement

313 The area and mean distance between mitochondria and myofilaments were  
314 automatically quantified (Fig.4). Results showed that both the area of cytoplasm  
315 between mitochondria and myofilaments within ICEUs (median 120700 (IQR 87490-  
316 155500)  $\text{nm}^2$  in control vs. 168600 (124100-236200)  $\text{nm}^2$  in IUGR,  $p=0.015$ ) (Fig. 4E)  
317 and the mean distance (105.7 (86.7-137.9) nm in control vs. 133.7 (104.7-182.3) nm in  
318 IUGR,  $p=0.037$ ) (Fig.4F) were significantly increased in IUGR rabbit myocardium.

319

### 320 3.3 Gene set expression analysis

321 All experiments showed a good level of labeling and hybridization onto the Agilent  
322 microarray. Genes were ordered by differential expression between the two  
323 experimental conditions and a ranked list with all genes of the experiment was obtained.  
324 We used the statistic of the statistical test for each gene, to order this list: genes at the  
325 top of list are more expressed in IUGR than in control group, and genes at the bottom  
326 are more expressed in control than IUGR group. Analyzing for a fold change higher  
327 than 0.5 and an adjusted p-value lower than 0.05 (data not shown), there were not genes  
328 with significant differential expression. The output result of the differential expression  
329 analysis (ranked list by the statistic of the test) was the input for the gene set analysis.  
330 On this full list of genes, Fatican detected groups of genes with the same expression  
331 pattern and sharing biological functions and extracted significantly under- and over-

332 represented Gene Ontology terms in a set of genes after comparing two sub-lists of  
333 genes with different pattern of expression: the first list included genes more expressed  
334 in IUGR group and the second list with genes more expressed in control group.  
335 Therefore, this analysis evaluated both the IUGR group and control group at the same  
336 time. Gene set analysis showed that IUGR subjects presented a statistically significant  
337 enrichment in groups of genes involved in energy production and cardiac energetic  
338 metabolism regulation (Table 2). Oxidative phosphorylation annotation (GO: 0006119,  
339 biological process) was found in 1.03% of the most up-regulated genes in IUGR (list 1,  
340 more expressed in IUGR than control group), while only 0.17% of the most down-  
341 regulated genes in IUGR contained the annotation (list 2, more expressed in control  
342 than IUGR group) (Table S1.A). Similarly, the annotations for oxygen homeostasis  
343 (GO: 0032364, biological process) (Table S1.B), mitochondrial respiratory chain  
344 complex I (GO: 0005747, cellular component) (Table S1.C) and NADH dehydrogenase  
345 (GO: 0003954, molecular function) (Table S1.D) were found in 0.49%, 0.44% and  
346 0.35% respectively, of the most up-regulated genes in IUGR, and only in 0.04%, 0%  
347 and 0% of the most down-regulated genes in IUGR, respectively. All p-values were  $\leq$   
348 0.001 and all adjusted p-values were  $< 0.08$ .

349

#### 350 **4. Discussion**

351 The study presented here shows an association between IUGR and a less organized  
352 intracellular arrangement of the cardiomyocyte organelles. The specific disarrangement  
353 of the ICEUs together with differences in the expression of key pathways for energy  
354 production, suggest an impairment of the energetic metabolism under IUGR. This study  
355 can contribute to explain the process of fetal cardiac programming and the global  
356 contractile dysfunction previously described in IUGR fetuses and children (12, 13, 14).

357 The experimental IUGR model used in this study is based on the selective ligation of  
358 the uteroplacental vessels in pregnant rabbit at 25 days of gestation until 30 days of  
359 gestation. The model mimics IUGR in human pregnancy, since it induces a combined  
360 restriction of oxygen and nutrients, taking into account the role of the placenta (16, 17).  
361 Different gestational ages as well as different degrees of ligation severity were  
362 previously tested for this experimental IUGR model, concluding that the condition that  
363 best reproduced human IUGR due to placental insufficiency is the selective ligation of  
364 the 40-50% of the uteroplacental vessels at 25 days of gestation (16). It is known that in  
365 rabbits, complete organogenesis has been achieved at 19.5 days of gestation (9). The  
366 two previous statements together with the aim to reproduce late IUGR occurring in the  
367 third trimester of human pregnancy (which is mainly caused by placental and maternal  
368 vascular factors), lead to the rationale of the ligation from 25 to 30 days of gestation  
369 (16, 8). The severity of the experimental IUGR model reproducing human IUGR  
370 condition due to placental insufficiency, with regard to mortality rate and hemodynamic  
371 changes has been previously described (16, 17). Cardiac function from IUGR kits is  
372 characterized by changes on cardiovascular Doppler parameters, with increased ductus  
373 venosus pulsatility index and increased isovolumetric relaxation time (17). Here we  
374 present the biometric changes induced by the selective ligation of 40-50% of the  
375 uteroplacental vessels, which result, as expected, in lower birth and heart weights, as  
376 well as decreased crown-rump length and abdominal girth. Additionally, an increase in  
377 heart to body weight is denoted in IUGR, which could be interpreted as a hypertrophic  
378 compensatory mechanism and is consistent with previous studies from experimental  
379 models of severe IUGR (28, 54, 55).

380 Our current analysis reports cardiomyocyte structural changes induced by IUGR. The  
381 stereological estimation of the volume densities of the different cellular components  
382 evidences that IUGR fetal hearts show a less organized intracellular arrangement,

383 characterized by an increased relative volume occupied by cytoplasm and a decreased  
384 relative volume occupied by mitochondria. These changes under IUGR could be either  
385 due to alterations on cardiac development, hypoxia or to mechanical stress caused by  
386 pressure or volume overload (49, 53). All the above mechanisms are believed to occur  
387 in and contribute to the development of cardiac dysfunction in IUGR, although the  
388 exact mechanisms are still not well understood. Recently it has been shown that  
389 experimentally induced pressure overload results in a depression of mitochondrial  
390 respiratory capacity together with a reduction of total mitochondrial volume density,  
391 with a stronger effect on intermyofibrillar (IFM) compared to subsarcolemmal  
392 mitochondria (SSM) (42). Due to the fact that our study samples are fetal, we cannot  
393 provide structural and functional differences between IFM and SSM (32). Despite that,  
394 our observations of a decrease on mitochondrial relative volume in IUGR are in line  
395 with the observations from Schwarzer et al. (42) The resulting structural remodeling  
396 shown in Fig. 4 from Schwarzer et al. (42) appears to be very similar to the structural  
397 remodeling presented in this study in IUGR hearts (Fig.4). Additionally, in the same  
398 study (42), they relate a decrease in mitochondrial density with a decrease in  
399 mitochondrial size, since the citrate synthase activity is decreased in pressure overload  
400 but the mitochondrial number is not. We do not observe changes on the number or in  
401 the area of individual mitochondria. Since the stereological study shows a decreased  
402 relative volume occupied by mitochondria, we hypothesize that smaller mitochondrial  
403 size could be the reason for the decreased mitochondrial density (similar to what was  
404 described in pressure overloaded hearts (42)), despite the lack of significance, which  
405 might be attributed to sample size restrictions. The decrease in mitochondrial density  
406 but with no changes in myofibrillar content, as we show, has also been observed in fetal  
407 sheep subjected to high altitude hypoxia, which is in agreement with an alteration  
408 caused by the lack of oxygen during intrauterine life (27).

409 Concerning the relative volume occupied by cytoplasm, we observe that the total  
410 relative density of cytoplasm is increased in IUGR, however, when classifying it into  
411 free cytoplasm or cytoplasm within ICEUs, the former is not significantly increased  
412 while the later is increased in IUGR hearts. We show that both the area of cytoplasm  
413 and the mean distance between mitochondria and myofilaments within ICEUs are  
414 increased in IUGR myocardium. In fetal heart, energy transfer is believed to rely on the  
415 direct ATP and ADP channeling between organelles since the CK-bound (creatine  
416 kinase) system is not mature (23). Its efficiency mostly depends on the close interaction  
417 between mitochondria and myofilaments (24). In this regard, it has been reported that  
418 intracellular disorganization restricts ATP and ADP diffusion, decreasing the efficiency  
419 of energy transfer (5). Since ICEUs play a central role in maintaining cardiac energetic  
420 homeostasis, alterations on their structure could alter the energy production, utilization  
421 and transfer, and as a consequence, cardiac function could be compromised (45). Based  
422 on previous studies, our data suggests that ICEUs abnormal arrangement could  
423 contribute to the development of less efficient hearts in IUGR, maybe due to a decrease  
424 on the energy transfer efficiency from mitochondria to the main cardiac ATPases. Such  
425 compromise of cardiac function due to alterations on ICEUs has been previously  
426 evidenced in heart failure (24). The abnormal ICEUs arrangement in IUGR could also  
427 be interpreted as a maturation delay, as it has been described that during cardiac  
428 maturation there are major changes on the cardiomyocyte intracellular organization in  
429 which mitochondria get closer to myofilament to form the ICEUs (34).

430 Therefore, from one side our findings present a close similarity to the previously  
431 described in experimentally induced pressure overload cardiac dysfunction (18, 42). On  
432 the other side, it has been described that cytoarchitectural perturbations can lead to  
433 energetic alterations, and conversely perturbations of cellular energetic metabolism can  
434 lead to ultrastructural remodeling (52). In our study, it remains uncertain whether the



435 structural changes could contribute to be a cause or a consequence of the cardiac  
436 dysfunction previously documented in IUGR.

437 Subsequently, we wanted to evaluate whether these structural changes are related to  
438 subtle changes on gene expression. For this purpose we performed a gene expression  
439 microarray experiment, which is complementary to the structural data and provide new  
440 evidence regarding the insults that IUGR hearts are receiving. We have used advanced  
441 bioinformatics analytic tools based on FatiScan gene set analysis (3), integrated in  
442 Babelomics (31). We propose the use of such procedure to scan ordered lists of genes  
443 and understand the biological processes operating behind them. Genes were ordered by  
444 differential expression between two experimental conditions: IUGR and control. There  
445 were not individual genes with significant differential expression. The output result of  
446 the differential expression analysis (ranked list by the statistic of the test) was the input  
447 for the gene set analysis. On this full list of genes, Fatiscan detected groups of genes  
448 with the same expression pattern and sharing biological functions. Therefore, the same  
449 analysis evaluated IUGR group and control group at the same time. Our analysis  
450 identified key gene pathways related to cardiac energy production which were  
451 compromised under IUGR. This included oxygen homeostasis (GO: 0032364),  
452 oxidative phosphorylation (GO: 0006119), mitochondrial respiratory chain complex I  
453 (GO: 0005747) and NADH dehydrogenase activity (GO: 0003954). On one hand,  
454 alterations on the oxygen homeostasis and oxidative phosphorylation suggest that IUGR  
455 hearts are suffering from hypoxia. Previous studies have shown a 20-35% decrease in  
456 the oxidative phosphorylation in skeletal muscle from IUGR rats, leading to a decrease  
457 in ATP production and thus an impairment of skeletal muscle function (43).  
458 Additionally, exposure to chronic hypoxia has been related to a decrease in cardiac  
459 oxidative capacity in rats, which leads to a decline in ATP synthesis and in oxygen  
460 consumption (2). Hypoxia during early life has also been associated to persistent

461 changes in genes linked to the regulation of cardiac metabolic processes that remain  
462 present long after the termination of the neonatal hypoxic insult (15). This may  
463 eventually be linked to the cardiovascular programming due to IUGR and the long term  
464 persistence of the changes. On the other hand, alterations on the expression of  
465 mitochondrial respiratory chain complex I and specifically on the NADH  
466 dehydrogenase activity are again in line with the study of Schwarzer *et al.* in pressure  
467 overload, in which they observe decreased function of the mitochondrial respiratory  
468 chain complex I. Our observations are also consistent with other studies in human  
469 IUGR in which a deficiency of the mitochondrial respiratory chain complex I has been  
470 observed (19).

471 Several study limitations and technical considerations should be mentioned. The  
472 morphological characterization of cardiomyocyte intracellular organization and ICEUs  
473 only provides structural information. Further studies are required in order to elucidate  
474 the functional consequences of these alterations. The bioinformatics gene set analysis  
475 used in this study is useful for studying diseases in which subtle differences are  
476 expected to occur, like in IUGR. Therefore, rather than expression changes on  
477 individual genes, alterations are expected to occur at the level of biological pathways  
478 and functionally related groups of genes. IUGR is thought to be a multifactorial disease  
479 in which several pathways and multiple members of a pathway might be involved, often  
480 resulting in only subclinical changes. However, we acknowledge that is difficult to  
481 address the actual biological relevance of the gene expression findings. Future  
482 functional studies are required to relate the gene expression changes to the functional  
483 alterations at the cellular level. Finally, we do not evaluate the postnatal persistence in  
484 this study, which would provide valuable data of the long-term impact of the changes.  
485 However, this goal lies beyond the scope of the present study and it will be investigated  
486 in future research.

487 In conclusion we demonstrate that hearts from IUGR fetuses present a less organized  
488 intracellular arrangement of the cardiomyocyte organelles. These structural changes are  
489 accompanied with differences in the expression of groups of genes related to energy  
490 production and oxygen homeostasis. Overall, this study suggests that energetic  
491 metabolism is impaired in IUGR and provides new evidence to characterize cellular and  
492 subcellular mechanisms underlying cardiac remodeling in IUGR. Our findings might  
493 help to explain the global cardiac dysfunction previously documented in IUGR fetuses  
494 and children, and deserve further investigation to ascertain persistence on the long term  
495 as part of the cardiovascular programming observed in IUGR.

496

#### 497 **Acknowledgements**

498 Authors thank Dr Carmen López-Iglesias, head of the electron cryo-microscopy unit of  
499 CCiTUB (Centres Científics i Tecnològics de la Universitat de Barcelona) for her  
500 support and advice with electron microscopy techniques.

#### 501 **Grants**

502 This study was supported by grants from Ministerio de Economía y Competitividad PN  
503 de I+D+I 2008-2011 (ref. SAF2009\_08815); Instituto de Salud Carlos III (ref.  
504 PI11/00051, PI11/01709) cofinanciado por el Fondo Europeo de Desarrollo Regional de  
505 la Unión Europea “Una manera de hacer Europa”; Centro para el Desarrollo Técnico  
506 Industrial (Ref. cvREMOD 2009-2012) apoyado por el Ministerio de Economía y  
507 Competitividad y Fondo de inversión local para el empleo, Spain; and AGAUR 2009  
508 SGR grant nº 1099. I.T. was supported by a post-doctoral fellowship from Carlos III  
509 Institute of Health (Spain) (CD08/00176). P.G.C. acknowledges grant support to the  
510 Programa de Ayudas Predoctorales de Formación en Investigación en Salud del  
511 Instituto Carlos III, Spain (FI12/00362). A.G.T. was supported by an IDIBAPS (Institut  
512 d’Investigacions Biomèdiques August Pi i Sunyer) predoctoral fellowship.

**513 Disclosures**

514 No conflicts of interest, financial or otherwise, are declared by the authors.

515

516

517

518

519

520

521

522

523

524

525

526

527

528

529

530

531

532

533

534

535

536

537

538

## 539 REFERENCES

540

- 541 1. **Alberry M, Soothill P.** Management of fetal growth restriction. *Arch Dis Child*  
542 *Fetal Neonatal Ed* 92:F62-F67, 2007.
- 543 2. **Al Ghoulh I, Khoo NK, Knaus UG, Griendling KK, Touyz RM, Thannickal**  
544 **VJ, Barchowsky A, Nauseef WM, Kelley EE, Bauer PM, Darley-Usmar V,**  
545 **Shiva S, Cifuentes-Pagano E, Freeman BA, Gladwin MT, Pagano PJ.** Oxidases  
546 and peroxidases in cardiovascular and lung disease: new concepts in reactive  
547 oxygen species signaling. *Free Radic Biol Med* 51: 1271-1288, 2011.
- 548 3. **Al-Shahrour F, Arbiza L, Dopazo H, Huerta-Cepas J, Mínguez P, Montaner D,**  
549 **Dopazo J.** From genes to functional classes in the study of biological systems. *BMC*  
550 *Bioinformatics* 8: 114, 2007.
- 551 4. **Al-Shahrour F, Carbonell J, Minguez P, Goetz S, Conesa A, Tárrega J, Medina**  
552 **I, Alloza E, Montaner D, Dopazo J.** Babelomics: advanced functional profiling of  
553 transcriptomics, proteomics and genomics experiments. *Nucleic Acids Res* 36:  
554 W341-346, 2008.
- 555 5. **Anmann T, Guzun R, Beraud N, Pelloux S, Kuznetsov AV, Kogerman L,**  
556 **Kaambre T, Sikk P, Paju K, Peet N, Seppet E, Ojeda C, Tourneur Y, Saks V.**  
557 Different kinetics of the regulation of respiration in permeabilized cardiomyocytes  
558 and in HL-1 cardiac cells. Importance of cell structure/organization for respiration  
559 regulation. *Biochim Biophys Acta* 1757: 1597-1606, 2006.
- 560 6. **Bae S, Xiao Y, Li G, Casiano CA, Zhang L.** Effect of maternal chronic hypoxic  
561 exposure during gestation on apoptosis in fetal rat heart. *Am J Physiol Heart Circ*  
562 *Physiol* 285: H983-990, 2003.
- 563 7. **Barker DJ.** Fetal origins of cardiovascular disease. *Ann Med* 1: 3-6, 1999.
- 564 8. **Bassan H, Trejo LL, Kariv N, Bassan M, Berger E, Fattal A, Gozes I, Harel S.**  
565 Experimental intrauterine growth retardation alters renal development. *Pediatr*  
566 *Nephrol* 15:192-195, 2000.
- 567 9. **Beaudoin S, Barbet P, Barga F.** Developmental stages in the rabbit embryo:  
568 guidelines to choose an appropriate experimental model. *Fetal Diagn Ther* 18:422-  
569 427, 2003.
- 570 10. **Benjamini Y, Hochberg Y.** Controlling the false discovery rate a practical and  
571 powerful approach to multiple testing. *J R Statist Soc B* 57: 289-300, 1995.

- 572 11. **Breu H, Gil J, David Kirkpatrick D, Werman M.** Linear Time Euclidean  
573 Distance Transform Algorithms. *IEEE Trans Pattern Anal Mach Intell* 5: 529-533,  
574 1995
- 575 12. **Comas M, Crispi F, Cruz-Martinez R, Martinez JM, Figueras F, Gratacos E.**  
576 Usefulness of myocardial tissue Doppler vs. conventional echocardiography in the  
577 evaluation of cardiac dysfunction in early-onset intrauterine growth restriction. *Am J*  
578 *Obstet Gynecol* 203: e1-e7, 2010.
- 579 13. **Crispi F, Bijmens B, Figueras F, Bartrons J, Eixarch E, Le Noble F, Ahmed A,**  
580 **Gratacós E.** Fetal Growth Restriction Results in Remodeled and Less Efficient  
581 Hearts in Children. *Circulation* 121: 2427-2436, 2010.
- 582 14. **Crispi F, Hernandez-Andrade E, Pelsers MM, Plasencia W, Benavides-**  
583 **Serralde JA, Eixarch E, Le Noble F, Ahmed A, Glatz JF, Nicolaides KH,**  
584 **Gratacos E.** Cardiac dysfunction and cell damage across clinical stages of severity  
585 in growth-restricted fetuses. *Am J Obstet Gynecol* 199: e1-e8, 2008.
- 586 15. **Del Duca D, Tadevosyan A, Karbassi F, Akhavein F, Vaniotis G, Rodaros D,**  
587 **Villeneuve LR, Allen BG, Nattel S, Rohlicek CV, Hébert TE.** Hypoxia in early  
588 life is associated with lasting changes in left ventricular structure and function at  
589 maturity in the rat. *Int J Cardiol* 156: 165-173, 2012.
- 590 16. **Eixarch E, Figueras F, Hernández-Andrade E, Crispi F, Nadal A, Torre I,**  
591 **Oliveira S, Gratacós E.** An experimental model of fetal growth restriction based on  
592 selective ligation of uteroplacental vessels in the pregnant rabbit. *Fetal Diagn Ther*  
593 26: 203-211, 2009.
- 594 17. **Eixarch E, Hernandez-Andrade E, Crispi F, Illa M, Torre I, Figueras F,**  
595 **Gratacos E.** Impact on fetal mortality and cardiovascular Doppler of selective  
596 ligation of uteroplacental vessels compared with undernutrition in a rabbit model of  
597 intrauterine growth restriction. *Placenta* 32: 304-309, 2011.
- 598 18. **Friehs I, Cowan DB, Choi YH, Black KM, Barnett R, Bhasin MK, Daly C,**  
599 **Dillon SJ, Libermann TA, McGowan FX, del Nido PJ, Levitsky S, McCully JD.**  
600 Pressure-overload hypertrophy of the developing heart reveals activation of  
601 divergent gene and protein pathways in the left and right ventricular myocardium.  
602 *Am J Physiol Heart Circ Physiol* 304: H697-H708, 2013.
- 603 19. **Gibson K, Halliday JL, Kirby DM, Yapfilito-Lee J, Thorburn DR, Boneh A.**  
604 Mitochondrial oxidative phosphorylation disorders presenting in neonates: clinical  
605 manifestations and enzymatic and molecular diagnoses. *Pediatrics* 122: 1003-1008,  
606 2008.

- 607 20. **Gundersen HJ, Bendtsen TF, Korbo L, Marcussen N, Møller A, Nielsen K,**  
608 **Nyengaard JR, Pakkenberg B, Sørensen FB, Vesterby A, et al.** Some new,  
609 simple and efficient stereological methods and their use in pathological research and  
610 diagnosis. *APMIS* 96: 379-394, 1988.
- 611 21. **Hecher K, Snijders R, Campbell S, Nicolaidis K.** Fetal venous, intracardiac, and  
612 arterial blood flow measurements in intrauterine growth retardation: relationship  
613 with fetal blood gases. *Am J Obstet Gynecol* 173: 10-15, 1995.
- 614 22. **Hiraumi Y, Iwai-Kanai E, Baba S, Yui Y, Kamitsuji Y, Mizushima Y,**  
615 **Matsubara H, Watanabe M, Watanabe K, Toyokuni S, Matsubara H,**  
616 **Nakahata T, Adachi S.** Granulocyte colony-stimulating factor protects cardiac  
617 mitochondria in the early phase of cardiac injury. *Am J Physiol Heart Circ Physiol*  
618 29:H823-832, 2009.
- 619 23. **Hoerter JA, Kuznetsov A, Ventura-Clapier R.** Functional development of the  
620 creatine kinase system in perinatal rabbit heart. *Circ Res* 69: 665-676, 1991.
- 621 24. **Joubert F, Wilding JR, Fortin D, Domergue-Dupont V, Novotova M, Ventura-**  
622 **Clapier R, Veksler V.** Local energetic regulation of sarcoplasmic and myosin  
623 ATPase is differently impaired in rats with heart failure. *J Physiol* 586: 5181-5192,  
624 2008.
- 625 25. **Kanaka-Gantenbein C.** Fetal origins of adult diabetes. *Ann N Y Acad Sci* 1205: 99-  
626 105, 2010.
- 627 26. **Lemieux H, Semsroth S, Antretter H, Höfer D, Gnaiger E.** Mitochondrial  
628 respiratory control and early defects of oxidative phosphorylation in the failing  
629 human heart. *Int J Biochem Cell Biol* 43: 1729-1738, 2011.
- 630 27. **Lewis AM, Mathieu-Costello O, McMillan PJ, Gilbert RD.** Quantitative electron  
631 microscopic study of the hypoxic fetal sheep heart. *Anat Rec* 256:381-388, 1999.
- 632 28. **Lim K, Zimanyi MA, Black MJ.** Effect of maternal protein restriction during  
633 pregnancy and lactation on the number of cardiomyocytes in the postproliferative  
634 weanling rat heart. *Anat Rec (Hoboken)* 293: 431-437, 2010.
- 635 29. **Lopaschuk GD, Jaswal JS.** Energy metabolic phenotype of the cardiomyocyte  
636 during development, differentiation, and postnatal maturation. *J Cardiovasc*  
637 *Pharmacol* 56: 130-140, 2010.
- 638 30. Mathworks 2007b, version 7.5.0.342; MATLAB, The MathWorks Inc., Natick,  
639 Massachusetts, USA.
- 640 31. **Medina I, Carbonell J, Pulido L, Madeira SC, Goetz S, Conesa A, Tárraga J,**  
641 **Pascual-Montano A, Nogales-Cadenas R, Santoyo J, García F, Marbà M,**

- 642 **Montaner D, Dopazo J.** Babelomics: an integrative platform for the analysis of  
643 transcriptomics, proteomics and genomic data with advanced functional profiling.  
644 *Nucleic Acids Res* 38: W210-W213, 2010.
- 645 32. **Nassar R, Reedy MC, Anderson PA.** Developmental changes in the ultrastructure  
646 and sarcomere shortening of the isolated rabbit ventricular myocyte. *Circ Res* 61:  
647 465-483, 1987.
- 648 33. **Nouette-Gaulain K, Malgat M, Rocher C, Savineau JP, Marthan R, Mazat JP,**  
649 **Sztark F.** Time course of differential mitochondrial energy metabolism adaptation  
650 to chronic hypoxia in right and left ventricles *Cardiovasc Res* 66: 132-140, 2005.
- 651 34. **Piquereau J, Novotova M, Fortin D, Garnier A, Ventura-Clapier R, Veksler V,**  
652 **Joubert F.** Postnatal development of mouse heart: formation of energetic  
653 microdomains. *J Physiol* 588: 2443-2454, 2010.
- 654 35. **Porter GA, Hom J, Hoffman D, Quintanilla R, de Mesy Bentley K, Sheu SS.**  
655 Bioenergetics, mitochondria, and cardiac myocyte differentiation. *Prog Pediatr*  
656 *Cardiol* 31: 75-81, 2011.
- 657 36. **Rasband WS.** ImageJ, U. S. National Institutes of Health, Bethesda, Maryland,  
658 USA, <http://imagej.nih.gov/ij/>, 1997-2011.
- 659 37. **Ream M, Ray AM, Chandra R, Chikaraishi DM.** Early fetal hypoxia leads to  
660 growth restriction and myocardial thinning. *Am J Physiol Regul Integr Comp*  
661 *Physiol* 295:R583-595, 2008.
- 662 38. **Rueda-Clausen CF, Morton JS, Davidge ST.** Effects of hypoxia-induced  
663 intrauterine growth restriction on cardiopulmonary structure and function during  
664 adulthood. *Cardiovasc Res* 81:713-722, 2009.
- 665 39. **Rueda-Clausen CF, Morton JS, Lopaschuk GD, Davidge ST.** Long-term effects  
666 of intrauterine growth restriction on cardiac metabolism and susceptibility to  
667 ischaemia/reperfusion. *Cardiovasc Res* 90:285-294, 2011.
- 668 40. **Saks V, Kuznetsov AV, Gonzalez-Granillo M, Tepp K, Timohhina N, Karu-**  
669 **Varikmaa M, Kaambre T, Dos Santos P, Boucher F, Guzun R.** Intracellular  
670 Energetic Units regulate metabolism in cardiac cells. *J Mol Cell Cardiol* 52: 419-  
671 436, 2012.
- 672 41. **Scheubel RJ, Tostlebe M, Simm A, Rohrbach S, Prondzinsky R, Gellerich FN,**  
673 **Silber RE, Holtz J.** Dysfunction of mitochondrial respiratory chain complex I in  
674 human failing myocardium is not due to disturbed mitochondrial gene expression. *J*  
675 *Am Coll Cardiol* 40: 2174-2181, 2002.



- 676 42. **Schwarzer M, Schrepper A, Amorim PA, Doenst T.** Pressure Overload  
677 Differentially Affects Respiratory Capacity in Interfibrillar and Subsarcolemmal  
678 Mitochondria. *Am J Physiol Heart Circ Physiol* 304: H529-H537, 2012.
- 679 43. **Selak MA, Storey BT, Peterside I, Simmons RA.** Impaired oxidative  
680 phosphorylation in skeletal muscle of intrauterine growth-retarded rats. *Am J*  
681 *Physiol Endocrinol Metab* 285: E130-137, 2003.
- 682 44. **Seppet EK, Eimre M, Anmann T, Seppet E, Peet N, Käämbre T, Paju K,**  
683 **Piirsoo A, Kuznetsov AV, Vendelin M, Gellerich FN, Zierz S, Saks VA.**  
684 Intracellular energetic units in healthy and diseased hearts. *Exp Clin Cardiol* 10:  
685 173-183, 2005.
- 686 45. **Seppet EK, Eimre M, Anmann T, Seppet E, Piirsoo A, Peet N, Paju K, Guzun**  
687 **R, Beraud N, Pelloux S, Tourneur Y, Kuznetsov AV, Käämbre T, Sikk P, Saks**  
688 **VA.** Structure-function relationships in the regulation of energy transfer between  
689 mitochondria and ATPases in cardiac cells. *Exp Clin Cardiol* 11: 189-194, 2006.
- 690 46. **Skilton MK, Evans N, Griffiths KA, Harmer JA, Celermajer D.** Aortic wall  
691 thickness in newborns with intrauterine growth restriction. *Lancet* 23: 1484-1486,  
692 2005.
- 693 47. **Soothill PW, Nicolaides KH, Campbell S.** Prenatal asphyxia, hyperlacticaemia,  
694 hypoglycaemia, and erythroblastosis in growth retarded fetuses. *BMJ* 294: 1051-  
695 1053, 1987.
- 696 48. **Stanley WC, Recchia FA, Lopaschuk GD.** Myocardial substrate metabolism in the  
697 normal and failing heart. *Physiol Rev* 85: 1093-1129, 2005.
- 698 49. **Tintu A, Rouwet E, Verlohren S, Brinkmann J, Ahmad S, Crispi F, van Bilsen**  
699 **M, Carmeliet P, Staff AC, Tjwa M, Cetin I, Gratacos E, Hernandez-Andrade**  
700 **E, Hofstra L, Jacobs M, Lamers WH, Morano I, Safak E, Ahmed A, le Noble F.**  
701 Hypoxia induces dilated cardiomyopathy in the chick embryo: mechanism,  
702 intervention, and long-term consequences. *PLoS One* 4: e5155, 2009.
- 703 50. **Tong W, Xue Q, Li Y, Zhang L.** Maternal hypoxia alters matrix metalloproteinase  
704 expression patterns and causes cardiac remodeling in fetal and neonatal rats. *Am J*  
705 *Physiol Heart Circ Physiol* 301: H2113-2121, 2011.
- 706 51. **Turan S, Turan OM, Salim M, Berg C, Gembruch U, Harman CR, Baschat**  
707 **AA.** Cardiovascular transition to extrauterine life in growth-restricted neonates:  
708 relationship with prenatal Doppler findings. *Fetal Diagn Ther* 33:103-109, 2013.
- 709 52. **Ventura-Clapier R, Garnier A, Veksler V, Joubert F.** Bioenergetics of the failing  
710 heart. *Biochim Biophys Acta* 1813: 1360-1372, 2011.

- 711 53. **Verburg, BO, Jaddoe VW, Wladimiroff JW, Hofman A, Witteman JC,**  
712 **Stegers EA.** Fetal hemodynamic adaptive changes related to intrauterine growth:  
713 the Generation R Study. *Circulation* 117: 649-659, 2008.
- 714 54. **Wang KC, Zhang L, McMillen IC, Botting KJ, Duffield JA, Zhang S, Suter**  
715 **CM, Brooks DA, Morrison JL.** Fetal growth restriction and the programming of  
716 heart growth and cardiac insulin-like growth factor 2 expression in the lamb. *J*  
717 *Physiol* 589: 4709-4722, 2011.
- 718 55. **Xu Y, Williams SJ, O'Brien D, Davidge ST.** Hypoxia or nutrient restriction during  
719 pregnancy in rats leads to progressive cardiac remodeling and impairs postischemic  
720 recovery in adult male offspring. *FASEB J* 20:1251-1253, 2006.
- 721
- 722
- 723
- 724
- 725
- 726
- 727
- 728
- 729
- 730
- 731
- 732
- 733
- 734
- 735
- 736
- 737
- 738
- 739

740 **FIGURE CAPTIONS**

741

742 **Figure 1. Electron micrograph showing an example of the delineation** used to  
743 automatically quantify the area of cytoplasm and the mean distance between  
744 mitochondria and myofilaments within ICEUs.

745

746 **Figure 2. Cytoarchitectural organization of cardiac myocytes.** Representative  
747 micrographs showing the typical organization of the intracellular space in control (**A**)  
748 and IUGR (**B**) fetal cardiomyocytes. While mitochondria are highly compacted and  
749 packed close to myofilaments in controls, they are looser packed showing an increased  
750 cytosolic space both within the mitochondrial network (\*\*\*) and between mitochondria  
751 and myofilaments (arrow heads) in IUGR. **C**, stereological measurements of fetal  
752 control and IUGR cardiomyocytes showing the relative volume occupied by  
753 myofilaments, mitochondria, free cytoplasm (Free), cytoplasm between mitochondria  
754 and myofilaments (ICEUs) and total cytoplasm (Total). \* $p < 0.05$ . Data in graphs are  
755 expressed as mean  $\pm$  SD. Magnification: 20000x. Scale bar=2  $\mu$ m. Mit (mitochondria),  
756 Myof (myofilaments), Cyto (cytoplasm), N (nucleus).

757

758 **Figure 3. Mitochondria area and number.** **A**, average area of individual  
759 mitochondria, estimated delineating each mitochondria as shown in Fig 2.A and B. **B**,  
760 average number of mitochondria. Data in graphs are expressed as mean  $\pm$  SD.

761

762 **Figure 4. Arrangement of ICEUs.** Representative micrographs showing an overview  
763 of a mitochondrial network surrounded by myofilaments in a control (**A**) and IUGR (**B**)  
764 fetal cardiomyocyte. Images **C** (control) and **D** (IUGR) are a detail of image **A** and **B**,  
765 respectively, showing delineated ICEUs. While in control myocardium mitochondria  
766 are closely apposed to myofilaments, the cytoplasmic space between mitochondria and  
767 myofilaments is greater in IUGR. **E** and **F**, show the quantification of the average area  
768 of cytoplasm and the mean distance between mitochondria and myofilaments within  
769 ICEUs, respectively. \* $p < 0.05$ . Data in graphs are expressed as mean  $\pm$  SD.  
770 Magnification: 20000x. Scale bar=2 $\mu$ m. Mit (mitochondria), Myof (myofilaments),  
771 Cyto (cytoplasm), N (nucleus).

772

773

774

775

776

777

778

779

780

781

782

783

784

785

786

787

788

789

790

## 791 TABLES

792 **Table 1. Biometry in experimental groups.** All values are median and interquartile  
 793 range. g: grams; cm: centimetres. Data are expressed as mean  $\pm$  SD. \* p-value < 0.05.  
 794

	Control	IUGR	P value
795 Birth weight (g)	49.24 $\pm$ 8.03	29,76 $\pm$ 5.99	0.000*
796 Heart weight (g)	0.43 $\pm$ 0.07	0.29 $\pm$ 0.07	0.001*
797 Heart/body weight (x100) (g)	0.84 $\pm$ 0.12	1.02 $\pm$ 0.11	0.009*
797 Placental weight (g)	3.86 $\pm$ 1.06	2.23 $\pm$ 0.37	0.028*
798 Crown-rump length (mm)	10.56 $\pm$ 0.46	8.94 $\pm$ 1.05	0.004*
798 Abdominal girth	7.47 $\pm$ 0.93	6.38 $\pm$ 0.65	0.048*

799

800

801

802

803 **Table 2. Gene set analysis with FatiScan.** Gene Ontology annotations involved in  
 804 energy production and cardiac energetic metabolism regulation with a statistically  
 805 significant enrichment in IUGR. \* adjusted p-value < 0.08.  
 806

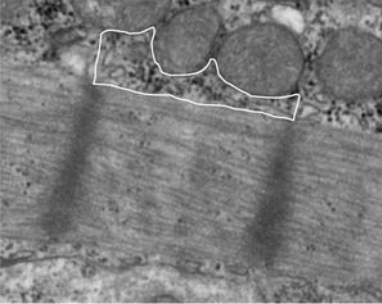
Annotation	Up- represented in IUGR	Down- represented in IUGR	p-value	adj. p- value	GO type
<b>Oxidative phosphorylation</b> (GO: 0006119)	1.03%	0.17%	1.15e-4	7.87e-2 *	Biological process
<b>Oxygen homeostasis</b> (GO: 0032364)	0.49%	0.04%	1.63e-4	7.82e-2 *	Biological process
<b>Mitochondrial respiratory chain complex I</b> (GO: 0005747)	0.44%	0%	1.39e-3	7.29e-2 *	Cellular component
<b>NADH dehydrogenase</b> (GO: 0003954)	0.35%	0%	4.37e-4	6.03e-2 *	Molecular function

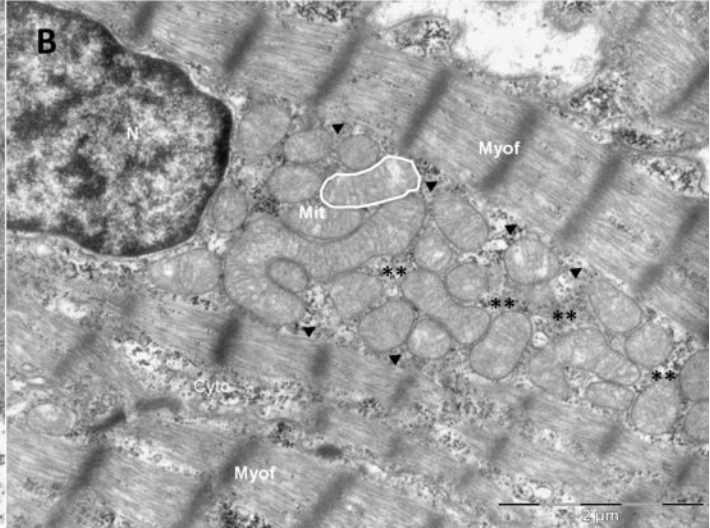
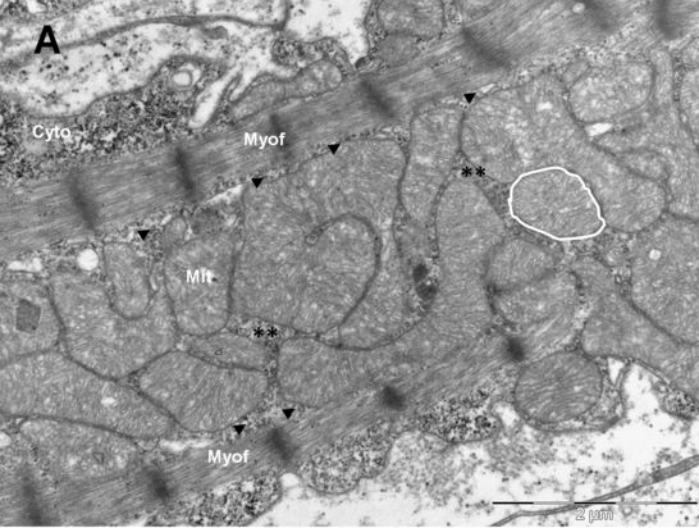
807

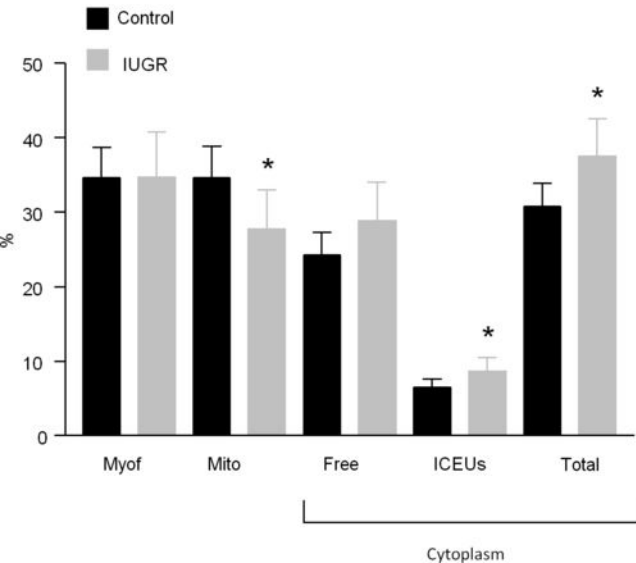
808

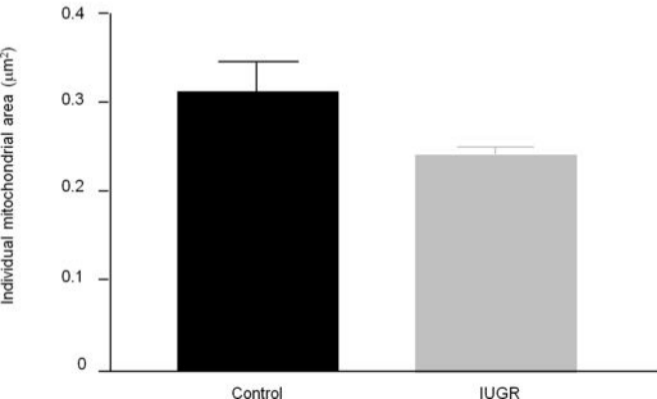
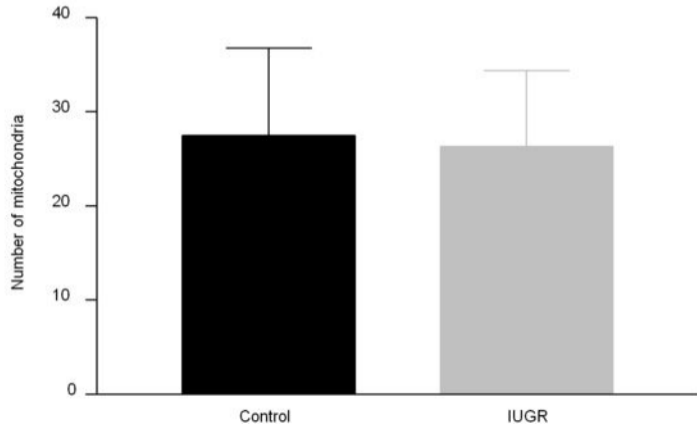
809

810

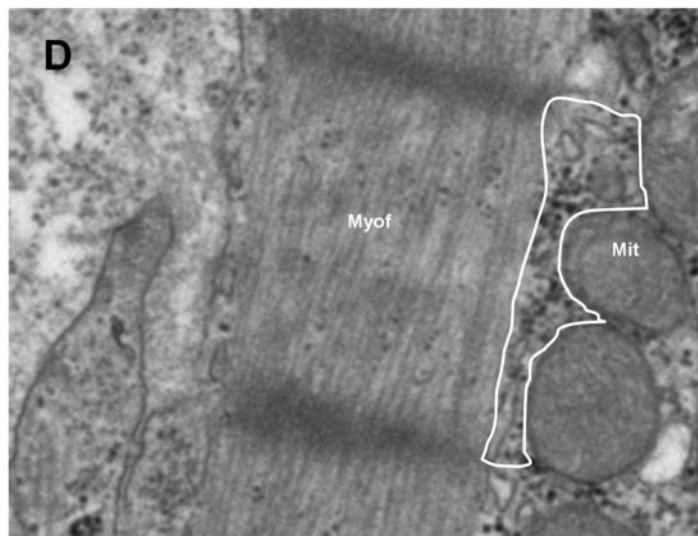
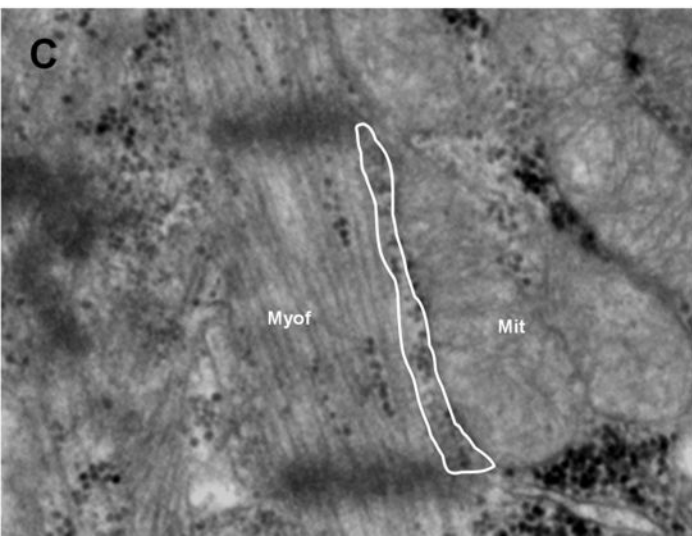
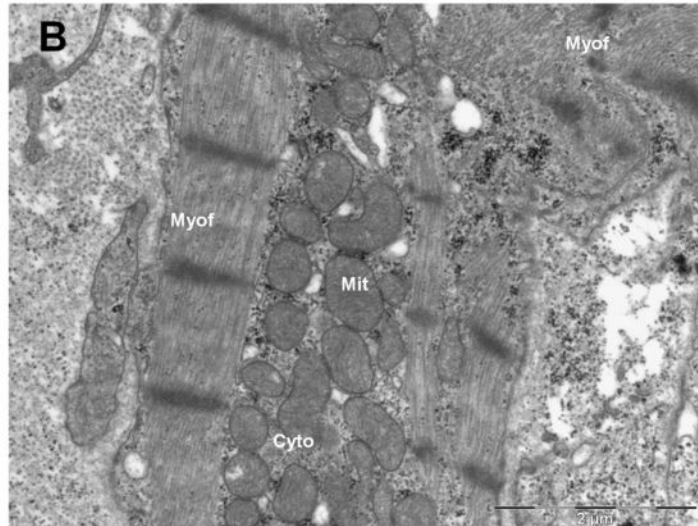
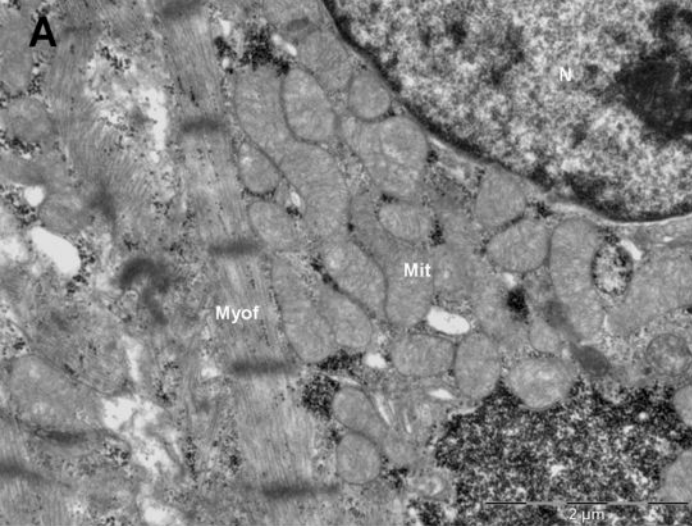


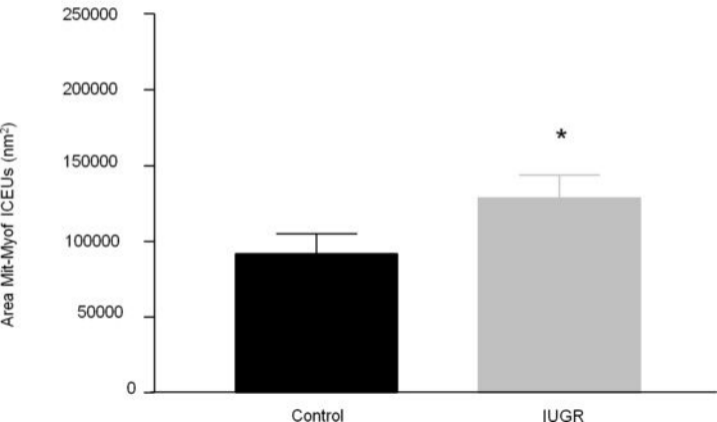


**C**

**A****B**





**E****F**